



Coherent Precession of an Individual $5/2$ Spin

M. Goryca,^{1,*} M. Koperski,¹ P. Wojnar,² T. Smoleński,¹ T. Kazimierzczuk,¹ A. Golnik,¹ and P. Kossacki¹

¹*Institute of Experimental Physics, University of Warsaw, ul. Hoża 69, 00-681 Warszawa, Poland*

²*Institute of Physics, Polish Academy of Sciences, al. Lotników 32/46, 02-688 Warszawa, Poland*

(Received 8 August 2014; published 25 November 2014)

We present direct observation of a coherent spin precession of an individual Mn^{2+} ion, having both electronic and nuclear spins equal to $5/2$, embedded in a CdTe quantum dot and placed in a magnetic field. The spin state evolution is probed in a time-resolved pump-probe measurement of absorption of the single dot. The experiment reveals subtle details of the large-spin coherent dynamics, such as nonsinusoidal evolution of states occupation, and beatings caused by the strain-induced differences in energy levels separation. Sensitivity of the large-spin impurity on the crystal strain opens the possibility of using it as a local strain probe.

DOI: 10.1103/PhysRevLett.113.227202

PACS numbers: 75.75.Jn, 42.50.Dv, 78.47.jb, 78.67.Hc

Coherent behavior of an individual spin in a solid has been demonstrated in several two- and three-level (so-called *lambda*) systems. Among them are systems such as a single electron [1–5], a hole [6], or an exciton [7,8] in a quantum dot (QD), a nitrogen-vacancy center in diamond [9,10], or a rare-earth ion in ceramic crystal [11]. However, coherence in more complex multilevel large-spin systems has been, up to now, inaccessible experimentally. A possibility to change this situation emerged due to constant progress in precise control of the doping of semiconductors. Within the past few years a whole new field of solotronics (solitary dopant optoelectronics) opened up [12], which is focused on the properties of individual ions and defects embedded in a semiconductor lattice. In particular, large-spin magnetic impurities have attracted a lot of interest. They offer desirable features of solitary spins, such as strong localization leading to weak coupling with a host crystal. Many experiments performed on different systems [13–15] provided substantial information on the physics of these objects, including the demonstration of optical readout and manipulation of the electronic spin state [16–18]. However, those experiments concerned only noncoherent phenomena. Coherent measurements, including observation of Rabi oscillations and a long coherence time, were performed only on ensembles of magnetic ions, e.g., colloidal QDs containing magnetic dopants [19], transition metal ions embedded in ZnO or MgO crystal [20–22], or ensembles of molecular magnets [23,24]. Up to now, the coherent dynamics of an individual large-spin particle has been considered only theoretically, showing, e.g., the possibility of using a molecular magnet for quantum information storage and processing [25,26] or a magnetic ion as a multiqubit system [27] with optical interface for readout and manipulation [28–30].

In this Letter we show a direct observation of a coherent spin precession of an individual Mn^{2+} ion, having both electronic and nuclear spins equal to $5/2$, placed in a magnetic field applied perpendicular to the quantization

axis of the system (see below). The idea of the experiment is to probe the spin state of the single Mn^{2+} ion in a time-resolved measurement of the absorption of a QD containing such an impurity. The QD is resonantly excited with two consecutive laser pulses, while the absorption is analyzed versus the relative delay between them.

The sample studied in the experiment contains a single layer of self-assembled CdTe/ZnTe QDs, grown by molecular beam epitaxy applying a similar growth procedure to that described in Refs. [31,32]. The dots are lens shaped, with the in-plane diameter ranging from 10 to 40 nm and the height-to-diameter ratio ranging from 1:5 to 1:3 [32]. They contain a low amount of Mn^{2+} ions, so that selection of single dots with exactly one magnetic ion is possible with the use of a microphotoluminescence setup. The emission of the QDs is excited either continuously with a rhodamine 6 G dye laser emitting in the range 570–610 nm or in a pulsed regime with an optical parametric oscillator (OPO) tuned to the same range. The pulses generated with OPO are spectrally narrowed and temporally broadened with the use of etalon. Its thickness determines the spectral and temporal width to about 0.6 meV and 1 ps, respectively. The OPO beam is split into two beams, one of which is passed through a mechanical delay line enabling precise control over the delay between the two pulses arriving at the sample.

The QD containing a single magnetic impurity is selected from the self-assembled system with the use of photoluminescence-excitation (PLE) measurements. The QD absorption is detected by using the excitation transfer to a neighboring dot from which the luminescence is recorded [17,33–35] [see Fig. 1(a)]. Excitons created resonantly in the dot containing the single magnetic ion do not recombine in this dot, as the transfer time to the coupled one is of the order of a few picoseconds [33], much shorter than their radiative lifetime. The recombination takes place in the coupled QD with a lower exciton ground energy, resulting in the emission of a photon at energy lower by about

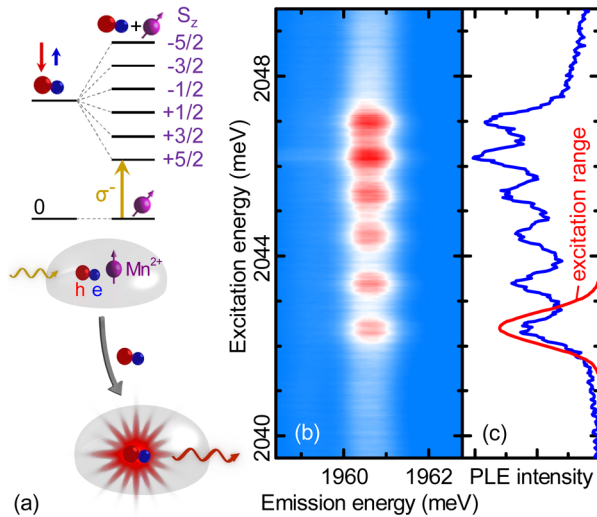


FIG. 1 (color online). (a) A schematic diagram of the excitation process of two coupled QDs with a single Mn^{2+} ion in the absorbing one together with a diagram of excitonic energy levels in a QD without and with such an ion, for $I_z = -1$ polarized exciton. Each optical transition in the dot with Mn^{2+} is related to a specific spin state of the ion. The arrow indicates the transition chosen for most of the experiments. (b) Photoluminescence excitation map (density plot of PL intensity versus emission and excitation photon energy) of the two coupled QDs. (c) Photoluminescence excitation spectrum of the QD with a single Mn^{2+} ion together with the spectrum of the pulsed laser used in time-resolved measurements.

100–200 meV than the excitation energy. The luminescence intensity of the emitting QD is monitored either at the neutral or at the charged exciton line, depending on the mean charge state of that dot. Such an approach assures a very short exciton lifetime in the absorbing QD, which is crucial for the temporal resolution of the experiment. A fingerprint of the presence of the single Mn^{2+} ion in the absorbing dot originates from the exciton- Mn^{2+} exchange interaction. Since the Mn^{2+} electronic spin is equal to $5/2$, this interaction leads to a sixfold splitting of the excitonic ground state [13]. As a result, six excitonic lines are visible in the absorption spectrum of the QD, which corresponds to six well separated bright spots on the PLE map, as shown in Fig. 1(b). In the time-resolved experiment, the pulsed laser is tuned to one of them. That leads to the formation of an exciton- Mn^{2+} complex with specifically chosen Mn^{2+} spin projection onto the growth axis (z), which defines the exciton quantization axis; see Fig. 1(a).

The measurements of the Mn^{2+} spin dynamics in the magnetic field are performed in a degenerate pump-probe regime, with both laser pulses exciting the transition corresponding to the same Mn^{2+} spin state. When the photon from the first pulse is absorbed by the QD, there is a little probability that during the lifetime of the exciton a scattering process takes place, leading to a change of the Mn^{2+} state. Such a process can involve, for example, an

exciton- Mn^{2+} spin flip-flop. As a result, after the pump pulse the Mn^{2+} spin state corresponding to the pumped transition is depleted as compared to the situation before the pulse. A similar process under continuous-wave excitation was already investigated and described in Ref. [36].

The second pulse probes the spin state of the Mn^{2+} ion. The probability of absorption is proportional to the probability of finding the ion in the state defined by the energy and polarization of the laser light. By measuring the absorption while varying the delay between the two pulses, we are able to probe the evolution of the selected Mn^{2+} spin state occupation. As the system under investigation is placed in a magnetic field not parallel to the quantization axis and is not in a relaxed state, one should expect to observe oscillation of the occupation of the state initially depleted by the pump pulse. The frequency of the oscillation is given by the magnetic field and Landé factor of the Mn^{2+} ion. The orientation of the magnetic field (perpendicular to the exciton quantization axis) is chosen to maximize the oscillation amplitude.

In order to have more complete insight into the complex spin evolution of the large-spin Mn^{2+} ion, the experiment is also performed in a nondegenerate regime. The pump and probe pulses are resonant with transitions corresponding to different spin states of the Mn^{2+} ion. In principle, this can be realized either by the use of different energies for the two pulses or the same energies but different circular polarizations. In our experimental setup the latter approach is used.

The pump-probe experiment is performed for several pairs of coupled QDs. Representative results are shown in Figs. 2(a)–2(c). The series of graphs shows the luminescence intensity of the emitting QD, coupled to the one containing the single Mn^{2+} ion, measured as a function of delay between the two laser pulses. The signal measured upon application of low magnetic field ($B = 0.6$ T) is presented in Fig. 2(a). The two curves represent data measured in a degenerate and a nondegenerate regime. In the first case, both pump and probe pulses correspond to the $S_z = +5/2$ state of the Mn^{2+} ion. In the second one, the pump pulse is adjusted to the $S_z = +5/2$ state, while the probe pulse is adjusted to the $S_z = -5/2$ state. Oscillations of the measured signal are clearly visible, indicating the coherent Larmor precession of the individual magnetic ion. The two curves present the same frequency of the oscillations, but an opposite phase, as expected for measurements in degenerate and nondegenerate regime.

Experimental data obtained for higher values of magnetic field are presented in Figs. 2(b) and 2(c). The frequency of the oscillations increases with the magnetic field and, as shown in the Fig. 2(f), follows the linear dependence on the field. The Landé factor of the Mn^{2+} ion deduced from this dependence is equal to 2.0. The amplitude of the oscillations clearly decreases for longer

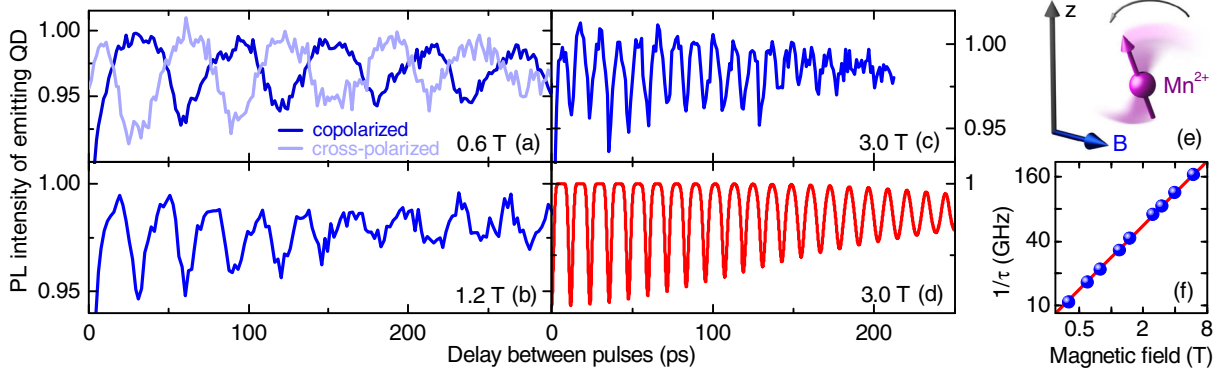


FIG. 2 (color online). (a)–(c) Measured and (d) calculated evolution of the occupation of the $S_z = +5/2$ state of the Mn^{2+} ion embedded in a QD for indicated values of magnetic field applied in Voigt configuration (perpendicularly to the quantization axis of the system). At magnetic field equal to 0.6 T, the signal is measured for both copolarized and cross-polarized pump and probe pulses. (e) A schematic diagram of Larmor precession of the Mn^{2+} spin in the magnetic field (B) applied perpendicularly to the quantization axis (z), given by the anisotropy of the exciton confined in the QD. (f) Dependence of the measured Larmor precession frequency on the magnetic field (points) together with linear fit (solid line).

delays, with characteristic time of about 200 ps and with no evidence of magnetic field dependence.

The complex properties of the 5/2 spin are revealed when analyzing in detail the occupation evolution of its spin states. It is not described with the simple sine curve. In particular, measured curves expose the subtle differences between the occupation evolution of different states of the

magnetic impurity. An example result presenting such differences is shown in Fig. 3(a). It compares two experimental curves taken with both pump and probe pulses tuned to the transitions related to the $S_z = +5/2$ or $S_z = +3/2$ states.

Experimental data representing the Mn^{2+} spin evolution can be quantitatively described taking into account the Zeeman effect for the electronic spin, the hyperfine coupling, the cubic crystal field, and the biaxial strain, which is usually a dominant strain component in CdTe QDs grown on ZnTe. This gives the following Hamiltonian [37,38]:

$$\mathcal{H} = g\mu_B \vec{B} \cdot \vec{S} + A \vec{I} \cdot \vec{S} + D_0 \left[S_z^2 - \frac{S(S+1)}{3} \right] + \frac{a}{6} \left[S_x^4 + S_y^4 + S_z^4 - \frac{S(S+1)(3S^2 + 3S - 1)}{5} \right], \quad (1)$$

where $g = 2.0$ is the Mn^{2+} Landé factor, $A = 680$ neV is the hyperfine coupling constant, $a = 320$ neV is the cubic crystal field splitting, and D_0 describes the effect of the biaxial strain component. Note that all of the above parameters are precisely known from EPR measurements of Mn^{2+} ions in bulk crystals [37], except for D_0 as it depends on the properties of a particular QD. Importantly, the term related to strain only slightly affects the precession frequency of the Mn^{2+} ion [37]. Therefore, its influence on the observed signal in a short time scale (of the order of 100 ps) can be neglected. In order to obtain the theoretical curve representing the occupation evolution of a selected spin state, we take the initially thermalized Mn^{2+} ion, deplete the state corresponding to the pump pulse energy at $t = 0$, and calculate the subsequent evolution of the ion spin state using the density matrix formalism. Additionally, for a comparison with the experimental data, such evolution

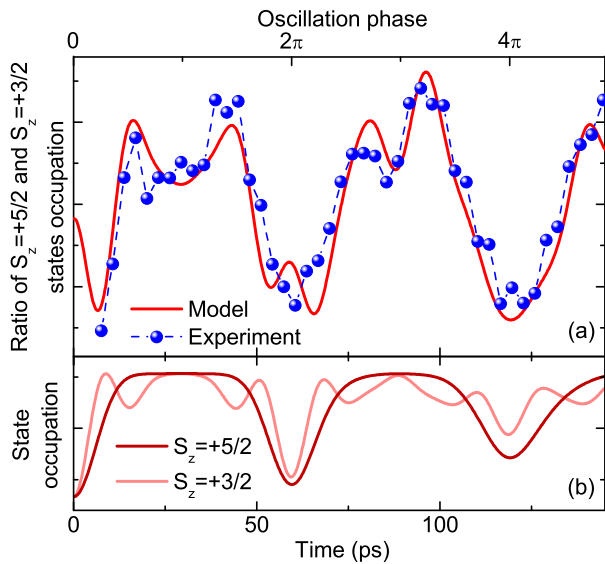


FIG. 3 (color online). (a) Measured (points) and calculated (solid line) curve representing the time-dependent ratio of the occupation of the $S_z = +5/2$ and $S_z = +3/2$ states of the Mn^{2+} ion in degenerate pump-probe measurements at $B = 0.6$ T. The theoretical curve obtained with the model described in the text (no fitting parameters except for vertical normalization) is convoluted with the Gaussian curve of the width equal to 3 ps, related to the experimental resolution. (b) Theoretical curves representing the occupation evolution of the $S_z = +5/2$ and $S_z = +3/2$ states before convolution with the Gaussian curve.

is convoluted with the Gaussian curve of the width equal to 3 ps, related to the overall experimental resolution.

As shown in Fig. 3(a), the difference between the two signals related to the $S_z = +5/2$ and $S_z = +3/2$ states is clearly reproduced with the theoretical curve. Note that, as we consider roughly the first 100 ps of the system evolution, the theoretical curve is computed with no fitting parameters except for vertical normalization. The Hamiltonian used for calculation takes into account only the Zeeman effect, the hyperfine coupling, and the cubic crystal field.

The decrease of the oscillations amplitude for the time scale longer than 100 ps, visible in Figs. 2(a)–2(c) may, in principle, originate from two factors, the Mn^{2+} spin decoherence or the influence of interactions additional to the Zeeman effect, making the whole process more complicated than the simple Larmor precession. The latter case is more desirable not only from an application point of view, but it also opens the possibility of experimentally exploiting the Mn^{2+} coherence in a long time scale. Here we show that the observed Mn^{2+} dynamics can be fully described without taking into account any coherence loss. An example fit to the experimental curve shown in Fig. 2(c) is presented in Fig. 2(d). It is obtained with the model taking into account all Hamiltonian terms shown in Eq. (1). Two of them lead to the observed decrease of the oscillations amplitude: the interaction of the Mn^{2+} electronic spin with the nuclear one and the term describing the strain-induced component of the crystal field. As the total nuclear spin is equal to $5/2$, there are—as in the case of the electronic spin—six possible projections onto the quantization axis. The hyperfine interaction between the two spins acts on the electronic one as a small effective magnetic field. Therefore, the precession frequency of the electronic spin slightly depends on the nuclear spin orientation. On the other hand, the strain-induced component of the crystal field changes the energy separation between different pairs of the Mn^{2+} spin states [37]. Thus, it introduces additional components to the frequency spectrum of the Mn^{2+} precession. The relative importance of these two effects depends on the ratio between the A and D_0 parameters of the Hamiltonian. Both of them also lead to the presence of beatings in the observed evolution of the Mn^{2+} spin. Such beatings are indeed observed for delays between the pump and probe pulses as long as 1.8 ns, which is shown in Fig. 4(a). The Fourier transform of the observed signal reveals a broad structure centered at the frequency determined by the magnetic field (53.2 GHz at 1.9 T) of the width equal to about 4 GHz, clearly visible in Fig. 4(c). Such width corresponds to the energy splitting an order of magnitude larger than A . This indicates that the observed beatings are caused mainly by the crystal field, which is also the main limiting factor for the characteristic time of the initial decrease of the observed oscillations amplitude. The best fit to the experimental data, shown in

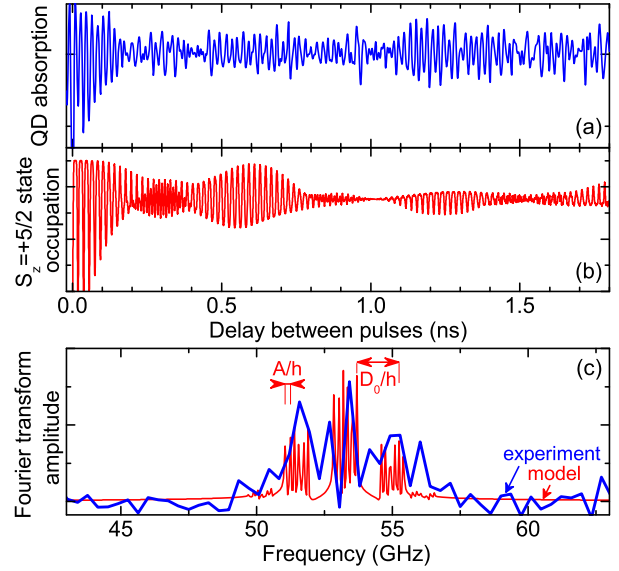


FIG. 4 (color online). (a) Measured and (b) calculated curve corresponding to the occupation evolution of the $S_z = +5/2$ state of the Mn^{2+} ion for large values of the delay between the pump and probe pulses, together with the Fourier transform of presented signals (c).

Fig. 4(b), is obtained using the parameter describing the strain component $D_0 = 6.5 \mu\text{eV}$. Such a value is close to $6 \mu\text{eV}$ previously reported for CdTe/ZnTe QDs [16] and about 2.5 times larger than the value reported for CdSe/ZnSe QDs [39], for which the D_0 parameter is expected to be smaller.

Because of experimental limitations, delays longer than 1.8 ns are not investigated. Nevertheless, the presence of coherence of the Mn^{2+} electronic spin after 1.8 ns permits us to regard this value as a lower bound of the T_2 time. The upper bound is given by the $2T_1$ measured previously on the same system, which is of the order of a millisecond [17].

To conclude, using the pump-probe technique to perform a time-resolved measurement of the absorption of a single QD containing a single Mn^{2+} ion, we have directly shown a coherent precession of an individual $5/2$ spin placed in magnetic field. The multitude of large-spin ion energy levels entails new effects when compared to simple two-level systems. Those effects include, e.g., nonsinusoidal evolution of states occupation and beatings caused by the strain-induced differences in energy levels separation. The latter effect opens the possibility of tailoring the vicinity of the magnetic ion to control its coherent evolution or, on the other hand, using the large-spin impurity as a probe of a local strain [40,41].

This work was supported by the Polish National Science Center under decisions No. DEC-2011/02/A/ST3/00131, No. DEC-2012/07/N/ST3/03130, No. DEC-2012/07/N/ST3/03665, No. DEC-2013/09/B/ST3/02603, and

No. DEC-2013/09/D/ST3/03768, by the Polish Ministry of Science and Higher Education as research grant “Diamantowy Grant,” and by the Foundation for Polish Science (MISTRZ program). This project was carried out with the use of CePT, CeZaMat, and NLTK infrastructures financed by the European Union—the European Regional Development Fund within the Operational Programme “Innovative Economy.” We thank Sophia Economou and Łukasz Cywiński for fruitful discussion and Aleksander Bogucki, Wojciech Pacuski, Łukasz Kłopotowski, Michał Nawrocki, and Jan Suffczyński for help in manuscript preparation.

*Mateusz.Goryca@fuw.edu.pl

- [1] D. Loss and D. P. DiVincenzo, *Phys. Rev. A* **57**, 120 (1998).
- [2] F. H. L. Koppens, C. Buizert, K. J. Tielrooij, I. T. Vink, K. C. Nowack, T. Meunier, L. P. Kouwenhoven, and L. M. K. Vandersypen, *Nature (London)* **442**, 766 (2006).
- [3] M. Atatüre, J. Dreiser, A. Badolato, A. Högele, K. Karrai, and A. Imamoglu, *Science* **312**, 551 (2006).
- [4] D. Press, T. D. Ladd, B. Zhang, and Y. Yamamoto, *Nature (London)* **456**, 218 (2008).
- [5] J. Berezovsky, M. H. Mikkelsen, N. G. Stoltz, L. A. Coldren, and D. D. Awschalom, *Science* **320**, 349 (2008).
- [6] D. Brunner, B. D. Gerardot, P. A. Dalgarno, G. Wüst, K. Karrai, N. G. Stoltz, P. M. Petroff, and R. J. Warburton, *Science* **325**, 70 (2009).
- [7] T. H. Stievater, X. Li, D. G. Steel, D. Gammon, D. S. Katzer, D. Park, C. Piermarocchi, and L. J. Sham, *Phys. Rev. Lett.* **87**, 133603 (2001).
- [8] H. Kamada, H. Gotoh, J. Temmyo, T. Takagahara, and H. Ando, *Phys. Rev. Lett.* **87**, 246401 (2001).
- [9] F. Jelezko, T. Gaebel, I. Popa, A. Gruber, and J. Wrachtrup, *Phys. Rev. Lett.* **92**, 076401 (2004).
- [10] T. Gaebel *et al.*, *Nat. Phys.* **2**, 408 (2006).
- [11] P. Siyushev *et al.*, *Nat. Commun.* **5**, 3895 (2014).
- [12] P. M. Koenraad and M. E. Flatte, *Nat. Mater.* **10**, 91 (2011).
- [13] L. Besombes, Y. Léger, L. Maingault, D. Ferrand, H. Mariette, and J. Cibert, *Phys. Rev. Lett.* **93**, 207403 (2004).
- [14] A. Kudelski, A. Lemaître, A. Miard, P. Voisin, T. C. M. Graham, R. J. Warburton, and O. Krebs, *Phys. Rev. Lett.* **99**, 247209 (2007).
- [15] J. Kobak *et al.*, *Nat. Commun.* **5**, 3191 (2014).
- [16] C. Le Gall, L. Besombes, H. Boukari, R. Kolodka, J. Cibert, and H. Mariette, *Phys. Rev. Lett.* **102**, 127402 (2009).
- [17] M. Goryca, T. Kazimierzczuk, M. Nawrocki, A. Golnik, J. A. Gaj, P. Kossacki, P. Wojnar, and G. Karczewski, *Phys. Rev. Lett.* **103**, 087401 (2009).
- [18] M. Goryca, T. Kazimierzczuk, M. Nawrocki, A. Golnik, J. Gaj, P. Wojnar, G. Karczewski, and P. Kossacki, *Physica (Amsterdam)* **42E**, 2690 (2010).
- [19] S. T. Ochsenein and D. R. Gamelin, *Nat. Nanotechnol.* **6**, 112 (2011).
- [20] J. Tribollet, J. Behrends, and K. Lips, *Europhys. Lett.* **84**, 20009 (2008).
- [21] S. Bertaina, L. Chen, N. Groll, J. Van Tol, N. S. Dalal, and I. Chiorescu, *Phys. Rev. Lett.* **102**, 050501 (2009).
- [22] R. E. George, J. P. Edwards, and A. Ardavan, *Phys. Rev. Lett.* **110**, 027601 (2013).
- [23] A. Ardavan, O. Rival, J. J. L. Morton, S. J. Blundell, A. M. Tyryshkin, G. A. Timco, and R. E. P. Winpenny, *Phys. Rev. Lett.* **98**, 057201 (2007).
- [24] S. Bertaina, S. Gambarelli, T. Mitra, B. Tsukerblat, A. Muller, and B. Barbara, *Nature (London)* **453**, 203 (2008).
- [25] M. N. Leuenberger and D. Loss, *Nature (London)* **410**, 789 (2001).
- [26] L. Bogani and W. Wernsdorfer, *Nat. Mater.* **7**, 179 (2008).
- [27] A. Gün, S. Çakmak, and A. Gençten, *Quantum Inf. Process.* **12**, 205 (2013).
- [28] A. K. Bhattacharjee, *Phys. Rev. B* **76**, 075305 (2007).
- [29] D. E. Reiter, T. Kuhn, and V. M. Axt, *Phys. Rev. Lett.* **102**, 177403 (2009).
- [30] D. E. Reiter, T. Kuhn, and V. M. Axt, *Phys. Rev. B* **83**, 155322 (2011).
- [31] P. Wojnar, J. Suffczyński, K. Kowalik, A. Golnik, G. Karczewski, and J. Kossut, *Phys. Rev. B* **75**, 155301 (2007).
- [32] P. Wojnar, J. Suffczyński, K. Kowalik, A. Golnik, M. Aleszkiewicz, G. Karczewski, and J. Kossut, *Nanotechnology* **19**, 235403 (2008).
- [33] T. Kazimierzczuk, J. Suffczyński, A. Golnik, J. A. Gaj, P. Kossacki, and P. Wojnar, *Phys. Rev. B* **79**, 153301 (2009).
- [34] M. Goryca, P. Plochocka, T. Kazimierzczuk, P. Wojnar, G. Karczewski, J. A. Gaj, M. Potemski, and P. Kossacki, *Phys. Rev. B* **82**, 165323 (2010).
- [35] M. Koperski, M. Goryca, T. Kazimierzczuk, T. Smoleński, A. Golnik, P. Wojnar, and P. Kossacki, *Phys. Rev. B* **89**, 075311 (2014).
- [36] C. Le Gall, A. Brunetti, H. Boukari, and L. Besombes, *Phys. Rev. Lett.* **107**, 057401 (2011).
- [37] M. Quazzaz, G. Yang, S. Xin, L. Montes, H. Luo, and J. K. Furdyna, *Solid State Commun.* **96**, 405 (1995).
- [38] M. Goryca *et al.*, *Phys. Rev. Lett.* **102**, 046408 (2009).
- [39] P. G. Baranov, N. G. Romanov, D. O. Tolmachev, R. A. Babunts, B. R. Namozov, Yu. G. Kusrayev, I. V. Sedova, S. V. Sorokin, and S. V. Ivanov, *JETP Lett.* **88**, 631 (2009).
- [40] A. M. Yakunin *et al.*, *Nat. Mater.* **6**, 512 (2007).
- [41] S. Ithurria, P. Guyot-Sionnest, B. Mahler, and B. Dubertret, *Phys. Rev. Lett.* **99**, 265501 (2007).